Statistical Models of Shape and Spatial Relation-application to Hippocampus Segmentation

Saïd Ettaïeb[1], Kamel Hamrouni[1] and Su Ruan[2]

[1]*Université de Tunis El Manar, Ecole Nationale d'Ingénieurs de Tunis, Research Laboratory of Image,*
Signal and Information Technology, Tunis, Tunisia
[2]*LITIS-Quantif, University of Rouen, Rouen, France*

Keywords: Spatial Relations, Active Shape Model-ASM, Statistical a Priori Knowledge, MRI, Hippocampus.

Abstract: This paper presents a new method based both on Active Shape Model (ASM) and spatial distance model to segment brain structures. It combines two types of a priori knowledge: the structure shapes and the distances between them. This knowledge consists of shape and distance variability which are estimated during a training step. Then, the obtained models are used to guide simultaneously the evolution of initial structure shapes towards the target contours. The proposed models are applied to extract two hippocampal regions on coronal MRI of the brain. The obtained results are encouraging and show the performance of the proposed model.

1 INTRODUCTION

One of the main problems of medical images segmentation is that they often present several anatomical structures having no clear boudaries and whose appearance is very similar. The automatic separation of regions of interest is often a difficult task. In particular, the use of techniques based only on the low-level characteristics of the image is not reliable, because the intensity of a pixel cannot give certain information about its membership in a structure. A promising way to remove ambiguity and improve the performance of segmentation results is to exploit high-level a priori knowledge, related to the studied anatomical structures. Among this knowledge, there are the spatial relations between the structures in the same scene. These relations represent structural knowledge for an image. They are often more stable than the appearance characteristics of the structures themselves.

Thus, they can be advantageously used to improve the segmentation of medical images.

In this context, we propose to develop a new model based on the Active Shape Model-ASM (Cootes, 1995) and a spatial relation of distance. The objective is to define a robust model capable to segment two structures of interest simultaneously using two types of a priori knowledge: the shape of each structure and the distance between them. So, the idea is to take advantage of statistical a priori knowledge of shape and integrate a new knowledge about the variability of spatial distance relation between the structures to be segmented. This knowledge is represented by a statistical distance model estimated during a training step. The obtained model will be then used to guide the evolution of two initial shapes towards the target structures and guarantee the preservation of the distance between shapes in an authorized interval.

The proposed model is validated on a clinical application, where the problem consists in segmenting two structures of interest: two hippocampal regions (left and right) on coronal MRI of the brain.

This application represents a major interest in clinical practice for early diagnosis of Alzheimer's disease.

This paper is organized as follows. In Section 2, we present spatial relations and their previous use in medical images segmentation. Section 3 is devoted to the integration of a statistical distance model to guide the segmentation process. In Section 4, the proposed model is applied to extract two hippocampal regions on coronal MRI of the brain.

2 SPATIAL RELATIONS

Spatial relations can be defined as the set of "facts" that describe the location of objects in space. They are mainly expressed by prepositions, which connect several entities: "A is next to B", "A is near B", "A is on the right of B", "A is inside B", "A is in front of B "," A is behind B "," A is between B and C ", etc. Some authors like [Freeman in 1975, Borillo in 1998] tried to define standard vocabularies in order to describe the spatial relations. Generally, these relations can be classified in three main categories, considered as fundamental: the topological relations used to describe the adjacency between structures ("is adjacent to", "crosses ", "is included"), the distance relations representing the distance between structures ("close", "far", "to a distance of ") and the direction relations based on the six usual directions.

These relations represent interesting structural information to model and interpret a scene. In the medical field, the human body is a typical example of structured scenes. Several books of anatomy presented many linguistic descriptions involving spatial relations between anatomical structures of the body. It seems that the modeling and the use of these relations are an interesting way to remove ambiguity and constrain the segmentation procedures to be more reliable.

Among the first remarkable work available on this subject, we find that of Geraud (Geraud, 1998). He proposed a sequential method of recognition of brain structures, where every structure is recognized thanks to the structural information resulted from the previously recognized structures. This information is generated from relations of distance and direction defined with regard to the already segmented structures. In the same context, Bloch and al proposed, in (Bloch, 2003), a method where the segmentation is performed from the beginning in a zone of interest defined by the spatial relations. In (Perchant, 2002), Perchant proposed a procedure for recognition of brain structures based on the matching of graphs: a graph derived from a reference image manually segmented by an expert and a graph of the image to be recognized. On the graphs, the nodes are the structures of interest and the arcs are the spatial relations between these structures.

In the mentioned work, spatial relations are mainly used in the step of recognition of anatomical structures. The real segmentation is made with classic methods. As part of his thesis work (Colliot, 2003), Colliot presented a particularly interesting work, where spatial relations are used effectively in the segmentation step. Relations such as direction, distance and adjacency are represented by fuzzy sets and integrated into the evolution equation of the active contour (Kass, 1987) as an external force. For the segmentation of a given structure, this force attracts the curve towards the image areas where the considered spatial relations are verified. Other recent studies were also proposed (Hudelot, 2008, Fouquier, 2010), where spatial relations are used either in the stage of recognition or in the segmentation step.

Our contribution is in this context and with the same concept as the work proposed by Colliot and Al. Indeed, we propose to model statistically the spatial distance relation "A is at a distance of B" and to use it directly in the segmentation step. This relation will be expressed as a statistical distance model and will be then integrated into the segmentation procedure of ASM.

3 STATISTICAL MODEL OF SHAPE AND SPATIAL RELATION

The main idea is to combine the ASM with a priori knowledge about the variation of a spatial distance relation, in order to define a new statistical model of shape and spatial relation.

The proposed model requires two main steps:

- A Training step, which aims to deduce from the training set three elementary models: a statistical shape model for every structure and a statistical distance model which expresses the variation of the distance between them.

- A segmentation step, based on the obtained models to guide the simultaneous evolution of two initial shapes towards the two target structures.

3.1 Training Step

This step consists in collecting at first a set of samples of images reflecting the possible variations of two structures to be segmented. Then, we extract, from each image, the shape of each structure by placing a sufficient number of landmarks on the target contours. Considering that n and m are respectively the number of landmarks required to represent the details of the first and the second structure and N is the number of images in the training set, each structure can be represented by a matrix of points defined as follows:

$M_{struct_1}(\boldsymbol{2n}, N) =$

v_{11}	v_{21}	v_{i1}	v_{N1}
x_{111}	x_{211}	....	x_{N11}
y_{111}	y_{211}	....	y_{N11}
$\vdots$	$\vdots$	....	$\vdots$
x_{11n}	x_{21n}	....	x_{N1n}
y_{11n}	y_{21n}	....	y_{N1n}

$M_{struct_2}(\boldsymbol{2m}, N) =$

v_{12}	v_{22}	v_{i2}	v_{N2}
x_{121}	x_{221}	....	x_{N21}
y_{121}	y_{221}	....	y_{N21}
$\vdots$	$\vdots$	....	$\vdots$
x_{12m}	x_{22m}	....	x_{N2m}
y_{12m}	y_{22m}	....	y_{N2m}

with v_{ij} is the vector of points which models the structure j on the image i. (x_{ijk}, y_{ijk}) are the coordinates of the point k placed in the image i on the contour of the structure j. From these two matrices, the shape model of each structure and the corresponding distance model can be constructed.

3.1.1 Construction of Statistical Shape Models

The construction of a statistical shape model is described in detail in (Ghassan, 1998). Indeed, from two obtained matrices of points, we can calculate the mean shape relative to each structure:

$$\bar{V}_1 = \frac{1}{N} \sum_{i=1}^{N} v_{i1} \qquad (1)$$

$$\bar{V}_2 = \frac{1}{N} \sum_{i=1}^{N} v_{i2} \qquad (2)$$

After a step of shapes alignment and by applying the PCA, we can also determine the modes and the amplitudes of deformation of every shape. Each structure can be then defined by a shape model that describes its geometry and deformation modes. These models can be respectively defined by:

$$V_1 = \bar{V}_1 + P_1 b_1 \qquad (3)$$

$$V_2 = \bar{V}_2 + P_2 b_2 \qquad (4)$$

with:
P_1 and P_2 are respectively the matrices of the main deformation modes of the first and the second structure. b_1 and b_2 are two weight matrices which represent respectively the projection of the shape V_1 in the base P_1 and the shape V_2 in the base P_2.

3.1.2 Construction of the Statistical Distance Model

The construction of the statistical distance model is made at the same time as that of the shapes models. It first consists in calculating the distances between both structures of interest from the training images and then trying to deduce a compact and precise formulation, which describes the authorized distances.

Given an image i of the training set where both structures of interest are modeled respectively by the two following vectors:

$$v_{i1} = (x_{i11}, y_{i11}, x_{i12}, y_{i12}, \ldots, \boldsymbol{x_{i1j}, y_{i1j}}, \ldots, x_{i1n}, y_{i1n})$$

$$v_{i2} = (x_{i21}, y_{i21}, x_{i22}, y_{i22}, \ldots, \boldsymbol{x_{i2k}, y_{i2k}}, \ldots, x_{i2m}, y_{i2m})$$

$M_j(x_{i1j}, y_{i1j})$ and $M_k(x_{i2k}, y_{i2k})$ are any two points of the first and the second structure. The Euclidean distance between M_j and M_k is defined by:

$$d(M_j, M_k) = \sqrt{(x_{i1j} - x_{i2k})^2 + (y_{i1j} - y_{i2k})^2} \qquad (5)$$

If the Euclidean distance of each landmark of the first structure with all points of the second one is calculated, we can define a matrix of distances with positive coefficients of n rows and m columns:

$$D_i = d(M_j, M_k)_{\substack{1 \le j \le n \\ 1 \le k \le m}} \qquad (6)$$

The elementary distance d_i between the two structures of interest on an image i is chosen as the Euclidean distance between their two closest landmarks:

$$d_i(v_{i1}, v_{i2}) = d_i(v_{i2}, v_{i1}) = \min(D_i) \qquad (7)$$

Similarly, we can calculate the distances between both structures of interest through all the images of the training set. The result is a vector of dimension N:

$$v_d = (d_1, d_2, \ldots \ldots, d_i, \ldots \ldots, d_N) \qquad (8)$$

The objective now is to deduce a compact formulation that describes authorized distances. Indeed, from the vector v_d, we can calculate the following basic statistical parameters:

- the mean distance between two structures of interest :

$$d_m = \frac{1}{N} \sum_{i=1}^{N} d_i \qquad (9)$$

- the variance which measures the dispersion of elementary distances (d_i) around the mean distance:

$$V(v_d) = \frac{1}{N} \sum_{i=1}^{N} (d_i - d_m)^2 \qquad (10)$$

(The more the variance is high, the more the variation of the distance between structures from an image to another one is important).

- the standard deviation, which represents the mean of all the elementary distances around the mean distance:

$$\sigma = \sqrt{V(v_d)} \qquad (11)$$

Using these parameters, we can calculate the confidence interval around the mean, which includes a large percentage of the initial elementary distances. Usually, the most adopted degree of confidence is equal to 95.4%. This degree leads to a confidence interval, limited as follows:

$$[d_m - 2\,\sigma\,,\, d_m + 2\,\sigma] \qquad (12)$$

This means that if we consider a new image to be segmented, the distance between both structures of interest belongs to the interval at 95.4%. (NB: An increase of the degree of confidence leads to a spreading of the confidence interval and thus a decrease in precision). Finally, we can propose a compact formulation of the distance between structures defined as follows:

$$d = d_m + 2\varphi\,\sigma \qquad (13)$$

with φ is a real parameter in the interval $[-1\,,1]$.

The equation 13 defines then the desired statistical distance model. This model represents thus a priori knowledge on the variation of distance between structures. It can be effectively used in the localization phase, to constrain the evolution of the initial shapes. For that purpose, we should calculate at each iteration the parameter φ as a function of the current distance d_c (distance between the two shapes in the current iteration). Equation14.

$$\varphi = \frac{d_c - d_m}{2\,\sigma} \qquad (14)$$

There are then three possible cases:

$$\begin{cases} \text{If } \varphi \in [-1,1] \text{ Then valid distance} \\ \quad \text{If } \varphi > 1 \; Then \; \varphi \leftarrow 1 \\ \quad \text{If } \varphi < -1 \text{ Then } \varphi \leftarrow (-1) \end{cases} \qquad (15)$$

In this way, we can require that the distance between shapes will always be in the authorized interval. This allows avoiding the divergence and the collision of shapes during the evolution and increasing the accuracy of results.

3.1.3 Integration of Distance Constraint

The integration of the distance constraint during the evolution can be defined by the algorithm presented in Table 1.

Table 1: Limitation by distance constraint.

d_c : *current distance*, φ: *real parameter*, F_1 : *shape1*, F_2 : *shape2*, v , u : *real variables*, d_m : *mean distance*, σ: *standard deviation*
If $\varphi \in [-1,1]$ *Then valid distance*
$\quad$ *Else_if* $\varphi > 1$ *Then* # $(d_c > d_m + 2\sigma)$
$\qquad v = d_c - (d_m + 2\sigma)$
$\qquad F_1 = F_1 - v/2$
$\qquad F_2 = F_2 + v/2$
$\qquad$ *Else* # $(d_c < d_m - 2\sigma)$
$\qquad u = (d_m - 2\sigma) - d_c$
$\qquad F_1 = F_1 + u/2$
$\qquad F_2 = F_2 - u/2$
$\quad$ *End*
$\quad$ *End*

3.2 Segmentation Guided by Shapes Models and Distance Model

The segmentation phase consists in placing, first of all, two initial shapes (mean shapes of two target structures) on the image to be segmented: a shape F_1, close to the first structure and a shape F_2, close to the second structure. Then, every iteration is divided into two basic steps:

- First, the initial two shapes evolve independently of each other, according to the constraints imposed by the corresponding shapes models. The evolution of shapes is based on the luminance properties of the processed image. This provides two intermediate shapes $F_1{}'$ and $F_2{}'$.

- Then, we calculate the current distance d_c between $F_1{}'$ and $F_2{}'$ and we estimate the real parameter φ. This allows applying the constraint imposed by the distance model (equation 15) and thus producing two new shapes with a valid distance between them.

This process is repeated until no significant changes are detected or the maximum number of iterations is reached. Thus, segmentation takes into account two essential information: the shape constraints related to each structure and a global constraint of distance between them. This localization phase can be simulated by the algorithm presented in Table 2.

Table 2: Segmentation guided by shapes models and distance model.

$$i = 0$$
Initialization _ shape1 : F_{1i}
Initialization_ shape2 : F_{2i}
While (convergence==no and
$i < nbr\_\text{max\_iterations})$

1. $F_{1i}^{'}$=*evolution_shape1(* F_{1i} *,* $V_1 = \bar{V}_1 + P_1 b_1$ *)*
2. $F_{2i}^{'}$=*evolution_shape2(* F_{2i} *,* $V_2 = \bar{V}_2 + P_2 b_2$ *)*
3. d_c=*distance (* $F_{1i}^{'}$ *,* $F_{2i}^{'}$ *)*
4. $(F_{1(i+1)}, F_{2(i+1)})$= *distance _limitation*
   $(d_c, F_{1i}^{'}, F_{2i}^{'}, d = d_m + 2\varphi\, \sigma$ *)*
5. *Convergence=compare (* $(F_{1i}, F_{1(i+1)})$
   $\&(F_{2i}, F_{2(i+1)}))$
6. $i=i+1$

End

4 APPLICATION TO HIPPOCAMPUS SEGMENTATION IN MRI

The hippocampus is a brain structure that is part of the cortex. This is a pair structure, which appears in an almost symmetrical way in each hemisphere. It is involved in several neurological diseases including Alzheimer's disease, which currently represents a major problem of the public health. In clinical practice, an early diagnosis of Alzheimer's disease is based, necessarily, on the detection of atrophy of hippocampal structures.

Many segmentation methods have been proposed to contribute to the quantification of hippocampal atrophy. Given the small size of this structure and the imprecision of its limits, the proposed methods are often based on a priori models (topology, texture, relative position, etc.). These models are derived from a statistical training set (Pizer, 2001 Pitiot, 2002, Yang, 2004) or an anatomical atlas [Shen, 2011]. Pure deformable models have been also used (Shen, 2002, Bailleul, 2007, Rajeesh, 2011). In (Babalola, 2008), the authors presented an interesting qualitative and quantitative comparison of four methods (Aljabar, 2007, Babalola, 2007 Patenaude, 2007, Murgasova, 2007) that were applied to the segmentation of internal brain structures on MRI, including the hippocampus.

The problems faced in these applications mostly come from poor anatomical definition of the hippocampus and the close similarity of its intensity with the surrounding tissues intensities. The isolation of hippocampal structures is often a difficult task. They are generally treated among other structures. In this work, we propose to contribute to the segmentation of hippocampal structures by relying on two types of a priori knowledge: a priori on the shape of each part separately (in each hemisphere) and a priori on the distance between them.

4.1 Qualitative Results

The application of our model requires first the construction of a training set. In this application, we used 18 MRI brain volumes. From each volume, we selected four T1-weighted coronal slices, where the hippocampal structures are represented. We thus obtained a set of 72 images of size 512*512 pixels. 50 images were used for the training and 22 images were reserved for the tests. In the training step, 30 landmarks are placed on each image: 15 points to extract the shape of the hippocampus in the right hemisphere, and 15 points to extract it in the left one. The variability percentage of the initial data is fixed to 95% and the length of the grey levels profile in the training step is 7 pixels. As a result, we ended up building a shape model for each part of the hippocampus and a distance model, which models the variation of the distance between them. The obtained parameters of the model are shown in Table 3.

Table 3: Parameters of shapes models and distance model.

	hippocampus (right part)	Hippocampus (left part)
Shapes models	7 principal variation modes	6 principal variation modes
Distance model	Mean distance $d_m = 62.26$, Standard deviation : $\sigma =14.19$	

In the localization phase, the initializations used in the various tests are calculated, each time, according to the mean shapes obtained during the training. The maximum number of iterations is fixed to 60 and the length of the search profile is 19 pixels.

Figure 1 shows an example of the localization result of the hippocampal structures, by presenting the effect of the distance constraint in intermediate iterations. Figure 2 shows the corresponding result by ignoring the distance constraint (using the same conditions).

The intermediate results in iteration 1 and iteration 10 (Figure 1) show that the application of the distance constraint helped to push positively the shapes to the regions of interest. This explains the remarkable difference between the accuracy of the

Initialisation

Iteration 1

Before limitation by distance constraint

After limitation by distance constraint

Iteration 10

Before limitation by distance constraint

After limitation by distance constraint
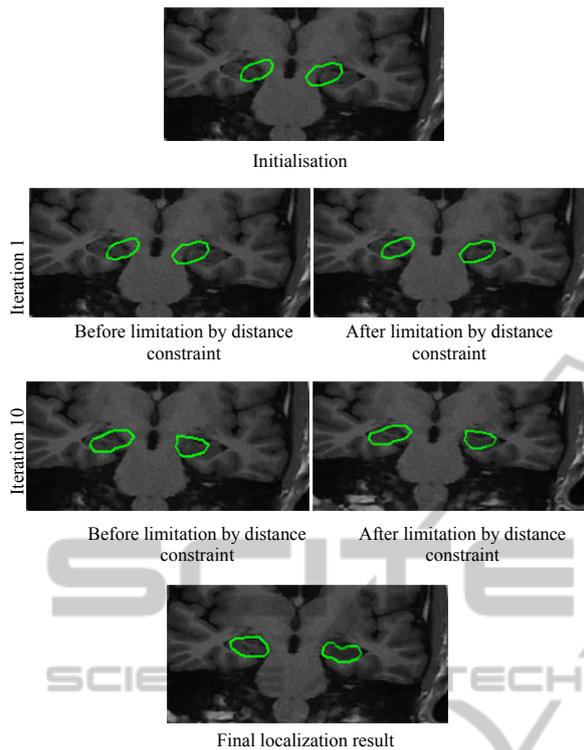
Final localization result

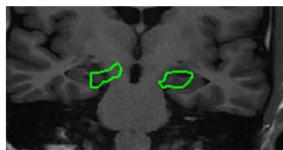Figure 1: Result of the segmentation of the hippocampal structures by ASMD

Figure 2: Result of the segmentation by ignoring the distance constraint.

final result by ASMD (our contribution) and that obtained by ignoring the distance constraint.

Figure 3 shows some segmentation results obtained on patients with different stages of hippocampal atrophy. We can notice that the initial shapes succeeded in capturing the hippocampal structures with different levels of atrophy. Thus, qualitatively, we can conclude that the results obtained by the proposed model for the segmentation of the hippocampus on MRI slices are satisfactory.
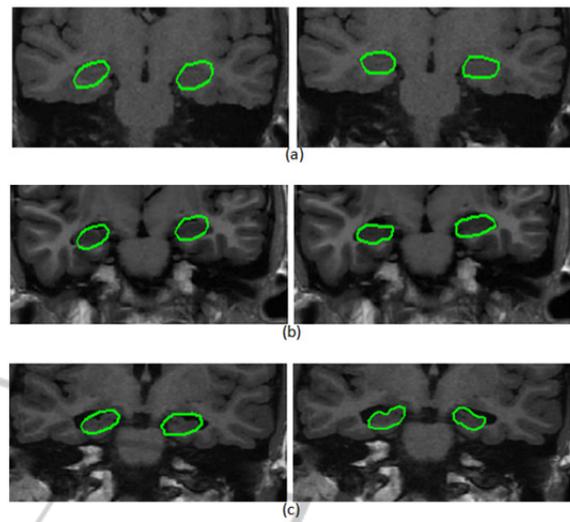

Figure 3: Examples of results obtained on patients with different stages of hippocampal atrophy. The first column shows the initializations and the second column shows the corresponding results. (a) case of healthy patient (b) case of patient with a mid-stage of atrophy (c) case of patient with a late stage of atrophy.

4.2 Quantitative Results

For the quantitative evolution, first, ten slices of the test database are selected and manually pre-segmented in order to be used as references. This ground truth is built with the help of an expert. Then we decided to compare our contribution ASMD with the ground truth, the original model of the ASM (without distance constraint) and another method proposed by Babalola and Al (Babalola, 2007). This latter, abbreviated PAM, is a variant of Active Appearance Model-AAM (Cootes, 1998) whose texture model is based on perpendicular profiles in the limits of the structure to be segmented and not on all its shape. The results of this comparison are presented in figure 4. It illustrates, by graph, the distance of Hausdorff between every method (ASMD, ASM and PAM) and the ground truth.

We can note that the Hausdorff distances found by ASMD for both parts of the hippocampus, vary from 2.81 (mm) to 5.14 (mm) with a global average of 3.74 (mm). These measures are lower than those found by the other two methods (ASM and PAM). We also note that both methods PAM and ASM in some cases give results close to the reference. However, they generate in other cases very different results even on the same slice. On the contrary, the results of ASMD have some stability and coherence between left and right part of almost all slices.

This is due to the fact that the segmentation of

both hippocampal structures, with ASMD, is made in a parallel and dependent way and is guided by two constraints: the shape and the distance. These results show the performance of the proposed model and the benefit of the integrated distance constraint. This additional constraint forced the initial curves to evolve regularly according to an acceptable distance and it thus channeled the evolution in the regions of interest.

Hippocampus (left part)

	i1	i2	i3	i4	i5	i6	i7	i8	i9	i10
ASM	7,82	8,02	6,13	9,36	11,5	8,92	10,1	9,04	7,28	7,87
PAM	4,85	5,02	4,25	4,02	6,13	5,93	7,12	4,26	5,45	4,23
ASMD	3,22	3,13	2,81	3,54	4,21	3,45	4,15	3,56	5	3,01

Hippocampus (right part)

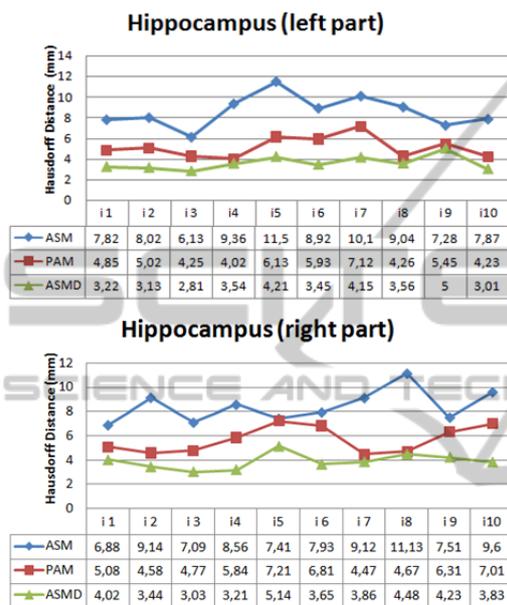|	i1	i2	i3	i4	i5	i6	i7	i8	i9	i10
ASM	6,88	9,14	7,09	8,56	7,41	7,93	9,12	11,13	7,51	9,6
PAM	5,08	4,58	4,77	5,84	7,21	6,81	4,47	4,67	6,31	7,01
ASMD	4,02	3,44	3,03	3,21	5,14	3,65	3,86	4,48	4,23	3,83

Figure 4: Results of the Hausdorff distance between the three methods (ASMD, ASM and PAM) and the ground truth.

In order to deduce the benefit of the integrated distance constraint relatively to the initialization, we made a comparison between the proposed ASMD model and the original model ASM compared to the ground truth. The comparison is performed on the same image with the same propagation conditions and by adopting different initializations. The results are shown in Figure 5. We can notice on the column 2 a clear difference between the quality of results. Indeed, for the three initializations, green curves (results obtained with ASMD) are closest to the red curves (reference segmentation). The second and the third initializations (shown respectively in the figure 5.b and 5.c) are placed relatively far from hippocampal structures. We see that, unlike the green curves (ASMD results), the purple curves (ASM results) fail to reach the regions of interest.

These results show that the used distance constraint partially solved the known problem of deformable models on initialization. It offers more flexibility during initialization.
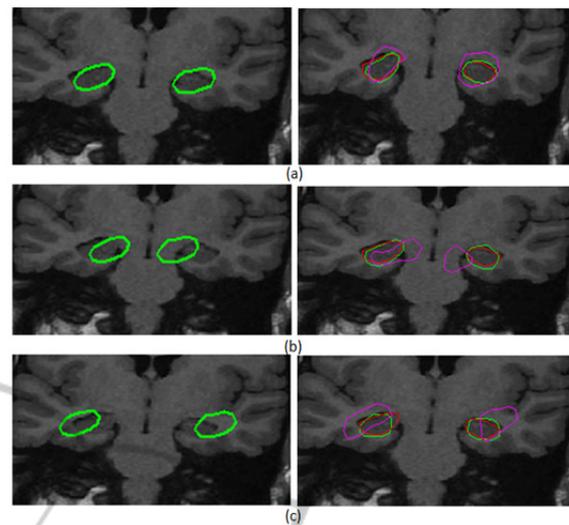

Figure 5: Comparison of results. The first column shows the different initializations. The second column shows the superposition of corresponding results: ASMD (green curves), ASM (purple curves) and the manual segmentation (red curves).

5 CONCLUSIONS

We presented an original segmentation model based on the ASM and a spatial distance relation. It allows the segmentation of two structures using two types of a priori knowledge: the shape of each structure and the distance between them. The proposed model is validated on a clinical application, where the problem is to segment two structures of interest: the extraction of two hippocampal regions (left and right) on coronal MRI of the brain. The obtained results are encouraging and show well the performance of the proposed model.

Although it showed its robustness and stability in the majority of tests, the proposed model has some limits and a number of perspectives that should be mentioned. First, the model is designed to segment two structures of interest, what limits the fields of its use. In addition, the integrated distance constraint is modeled by using the distances between the target structures independently from their positions in the image. Thus, theoretically and during the localization, the distance between shapes may be valid even if they are really far from the structures of interest. This may produce false results. Improvements in our model are then considered. Indeed, it is possible to increase its reliability by considering one of the two structures as a fixed reference and to model the distance variation according to this reference. This however requires a

prior segmentation of the structure that will be considered as a reference. The proposed model can easily be extended to segment several structures. It means, for example, considering the simplest structure to be segmented as reference and to segment the others with regard to this reference.

REFERENCES

Cootes, T. F., Taylor, C. J., Cooper, D. H., and Graham J., 1995. Active Shape Models - Their Training and Application. *Computer Vision and Image Understanding, vol.61, pp38-59.*

Freeman, J., 1975. The modeling of spatial relations. *Computer Graphic and image processing, Vol. 4, pp. 156-171.*

Borillo, A., 1998. L'espace et son expression en français. *Ophrys, Paris.*

Geraud, T., 1998. Segmentation des structures internes du cerveau en imagerie par résonnance magnétique tridimensionnelle. *Thèse de Doctorat, Télécom paris.*

Bloch, I., Géraud, T., and Maître, H., 2003. Representation and fusion of heterogeneous fuzzy information in the 3d space for model-based structural recognition-application to 3d brain imaging. *Artificial Intelligence, Vol. 148, pp. 141–175.*

Perchant, A., and Bloch, I., 2002. Fuzzy Morphisms between Graphs. *Fuzzy Sets and Systems, Vol. 128, pp. 149–168.*

Colliot, O, 2003. Représentation, évaluation et utilisation de relations spatiales pour l'interprétation d'images. Application à la reconnaissance de structures anatomiques en imagerie médicale. *Thèse de doctorat, Telecom Paris.*

Kass, M., Witikin, A., and Terzopoulos, D., 1987. Snakes: Active contour models. *International Journal of Computer vision, vol.1, pp. 321-331.*

Hudelot, C., Atif, J., and Bloch, I., 2008. Fuzzy Spatial Relation Ontology for Image Interpretation. *Fuzzy Sets and Systems, 159:1929–1951.*

Fouquier, G., 2010. Optimisation de séquences de segmentation combinant modèle structurel et focalisation de l'attention visuelle. Application à la reconnaissance de structures cérébrales dans des images 3D. *Thèse de doctorat, Ecole Nationale Supérieure des Télécommunications.*

Ghassan, H., 1998. Active Shape Models - Part I: Modelling Shape and Gray Level Variations. *Proceedings of the Swedish Symposium on Image Analysis.*

Pizer, S. M., Joshi, S., Thomas Fletcher, P., Styner, M., Tracton, G., and Chen, J. Z., 2001. Segmentation of Single-Figure Object by Deformable M-reps. *MICCAI, vol.2208, pp.862-871.*

Pitiot, A., Toga, A. W., and Thompson, P. M., 2002. Adaptive Elastic Segmentation of Brain MRI via Shape-Model-Guided Evolutionary programming. *IEEE TMI, vol.21, pp.910-923.*

Yang, J., Staib, L. H., and Duncan, J. S., 2004. Neighbor-Constrained Segmentation With Level Set Based 3-D Deformable Models. *IEEE TMI, vol.23, pp.940-948.*

Shen, K., 2011. Automatic Segmentation and Shape Analysis of Human Hippocampus in Alzheimer's Disease. *Thèse de Doctorat, Université De Bourgogne.*

Shen, D., Moffat, S., Resnick, S. M., and Davatzikos, C., 2002. Measuring Size and Shape of the Hippocampus in MR Images Using a Deformable Shape Model. *Neuroimage, Vol.15-2, pp.422-434.*

Bailleul, J., Ruan, S., and Constans, J. M., 2007. Statistical Shape Model-based Segmentation of brain MRI Images. *International Conference of the IEEE EMBS, Lyon, France, 2007.*

Rajeesh, J., Moni, R. S., and Palanikumar, S., 2001. A versatile algorithm for the automatic segmentation of hippocampus based on level set. *International Journal of Biomedical Engineering and Technology.*

Babalola, K. O., Patenaude, B., Aljabar, P. , Schnabel, J., Kennedy, D., Crum, W., Smith, S., Cootes, T. F., Jenkinson, M., and Rueckert, D., 2008. Comparison and Evaluation of Segmentation Techniques for Subcortical Structures in Brain MRI. *MICCAI.*

Aljabar, P., Heckemann, R., Hammers, A., Hajnal, J., and Rueckert, D., 2007. Classifier selection strategies for label fusion using large atlas databases. *MICCAI.*

Babalola , K. O., Petrovic, V., Cootes, T. F., Taylor, J. C., Twining, J. C., Williams, T. G., and Mills, A., 2007. Automated segmentation of the caudate nuclei using active appearance models. *In 3D Segmentation in the clinic: A grand challenge. Workshop Proceedings, MICCAI.*

Patenaude, B., Smith, S., Kennedy, D., and Jenkinson, M., 2007. Bayesian shape and appearance models. *Technical report TR07BP1, FMRIB Centre - University of Oxford.*

Murgasova, M., Dyet, L., Edwards, A. D., Rutherford, M., Hajnal, J., and Rueckert, D., 2007. Segmentation of brain MRI in young children. *Acad. Rad.*

Cootes, T. F., Edwards, G. J., and Taylor, C. J., 1998. Active appearance models. *European Conference on Computer Vision, pp 484–498.*